



HAL
open science

Simplified characteristic time method for accurate estimation of the soil hydraulic parameters from one-dimensional infiltration experiments

Mehdi Rahmati, Meisam Rezaei, Laurent Lassabatère, Renato Morbidelli,
Harry Vereecken

► **To cite this version:**

Mehdi Rahmati, Meisam Rezaei, Laurent Lassabatère, Renato Morbidelli, Harry Vereecken. Simplified characteristic time method for accurate estimation of the soil hydraulic parameters from one-dimensional infiltration experiments. *Vadose Zone Journal*, 2021, e20117, 10.1002/vzj2.20117. hal-03243379

HAL Id: hal-03243379

<https://univ-lyon1.hal.science/hal-03243379>

Submitted on 7 Nov 2022

HAL is a multi-disciplinary open access archive for the deposit and dissemination of scientific research documents, whether they are published or not. The documents may come from teaching and research institutions in France or abroad, or from public or private research centers.

L'archive ouverte pluridisciplinaire **HAL**, est destinée au dépôt et à la diffusion de documents scientifiques de niveau recherche, publiés ou non, émanant des établissements d'enseignement et de recherche français ou étrangers, des laboratoires publics ou privés.



Distributed under a Creative Commons Attribution - NonCommercial - NoDerivatives 4.0 International License

ORIGINAL RESEARCH ARTICLE

Simplified characteristic time method for accurate estimation of the soil hydraulic parameters from one-dimensional infiltration experiments

Mehdi Rahmati^{1,2} | Meisam Rezaei³ | Laurent Lassabatere⁴ | Renato Morbidelli⁵ | Harry Vereecken²

¹ Department of Soil Science and Engineering, University of Maragheh, Maragheh, Iran

² Forschungszentrum Jülich, Institute of Bio- and Geosciences: Agrosphere (IBG-3), Jülich, Germany

³ Soil and Water Research Institute (SWRI), Agricultural Research, Education and Extension Organization (AREEO), Karaj, Iran

⁴ University Lyon, Université Claude Bernard Lyon 1 CNRS, ENTPE, UMR5023 LEHNA, Vaulx-en-Velin F-69518, France

⁵ Department of Civil and Environmental Engineering, University of Perugia, Perugia, Italy

Correspondence

Mehdi Rahmati, Department of Soil Science and Engineering, University of Maragheh, Maragheh, Iran.

Email: mehdirmti@gmail.com

Harry Vereecken, Forschungszentrum Jülich, Institute of Bio- and Geosciences: Agrosphere (IBG-3), Jülich, Germany.

Email: h.vereecken@fz-juelich.de

Assigned to Associate Editor Hailong He

Abstract

Recently, a novel approach with excellent performance based on the concept of the characteristic infiltration time, the characteristic time method (CTM), is proposed to infer soil sorptivity (S) and saturated hydraulic conductivity (K_s) from one-dimensional (1D) cumulative infiltration. The current work provides a simplified version of the CTM, called the SCTM, by eliminating the necessity of the iteration method used in CTM and providing a similar accuracy as the original method when estimating S and K_s . We used both synthetic and experimental data to evaluate SCTM in comparison with the original CTM, as well as Sharma (SH) and curve-fitting methods. In the case of synthetically simulated infiltration experiments, the predicted S and K_s values showed an excellent agreement with their theoretical values, with Nash–Sutcliffe (E) values higher than 0.9 and RMSE values of $0.11 \text{ cm h}^{1/2}$ and 0.35 cm h^{-1} , respectively. In the case of experimental data, the SCTM showed E values larger than 0.73 and RMSE values of $0.64 \text{ cm h}^{1/2}$ and 0.35 cm h^{-1} , respectively. The accuracy and the robustness of SCTM was comparable with the original CTM when applied on synthetic infiltration curves as well as on experimental data. Similar to the original CTM, the simplified approach also does not require the knowledge of the time validity, which is needed when using approaches based on Philip's infiltration theory. The method is applicable to infiltrations with durations from 15 min to 24 h. The supplemental material presents the calculation of S and K_s using SCTM in an Excel spreadsheet.

1 | INTRODUCTION

Water infiltration plays a fundamental role in controlling, for example, surface runoff, groundwater recharge, the soil water available for evapotranspiration, and thus crop growth. Knowledge of the soil infiltration properties is also essential in managing irrigation systems and controlling soil salinity and

Abbreviations: 1D, one-dimensional; 3D, three-dimensional; CF2, nonlinear curve-fitting method of two-term equation; CF3, nonlinear curve-fitting method of three-term equation; CTM, characteristic time method; QEI, quasi-exact implicit; q-q, quantile–quantile; SCTM, simplified characteristic time method; SH, Sharma; SWIG, Soil Water Infiltration Global.

This is an open access article under the terms of the [Creative Commons Attribution](https://creativecommons.org/licenses/by/4.0/) License, which permits use, distribution and reproduction in any medium, provided the original work is properly cited.

© 2021 The Authors. *Vadose Zone Journal* published by Wiley Periodicals LLC on behalf of Soil Science Society of America

sodicity. Monitoring of infiltration rates under natural conditions is difficult if not impossible, and therefore the use of the hydrological models that correctly describe infiltration are very important.

Water infiltration into soils can either be described by using soil water balance models or by using theoretical, semiempirical, and empirical hydrological models (Corradini et al., 1997; Green & Ampt, 1911; Haverkamp et al., 1994; Parlange et al., 1982; Philip, 1957; Swartzendruber, 1987) for specific infiltration conditions. The former models are typically used for the characterization of soil sorptivity (S), a measurable physical quantity, which expresses the capacity of a porous medium to absorb or release liquids by capillarity (Philip, 1957), and saturated hydraulic conductivity (K_s), a measure of the soil's ability to transmit water under the influence of gravity.

In general, two major approaches are used to estimate S and K_s : linearization approaches (Sharma et al., 1980; Smiles & Knight, 1976; Vandervaere et al., 2000) and inverse estimation using curve-fitting method (Bonell & Williams, 1986; Bristow & Savage, 1987; Marquardt, 1963; Vandervaere et al., 2000). Both approaches usually result in very good agreement ($R^2 > .9$) between measured and predicted infiltration curves (Rahmati et al., 2020). However, linearization approaches suffer from substantial arbitrariness in deciding which part of the data fully meets linearity, leading to uncertainty in estimated infiltration parameters. On the other hand, the curve fitting methods suffer from equifinality, the principle that the minimum of the objective function can be obtained by a broad set of parameter values (Beven & Freer, 2001), as well as possible unrealistic parameter values when the optimization is unconstrained.

Rahmati et al. (2020) introduced a new procedure based on the use of the characteristic time (named characteristic time method, CTM) to predict S and K_s from one-dimensional (1D) infiltration experiments. Their method uses an iterative procedure to ensure accurate predictions of S and K_s regardless of the infiltration regime measured (i.e., the transient regime only or both transient and steady-state regimes). Contrary to previously published methods, the CTM does not require knowledge of the time validity of the applied semi-analytical solution for transient infiltration and can be applied to any infiltration duration (from a few minutes to several days). Rahmati et al. (2020) demonstrated the usefulness and strength of CTM in comparison with a suite of existing methods including classical methods of Sharma et al. (1980) (SH) and curve-fitting methods using two- (Haverkamp et al., 1994) (CF2) and three-term (Rahmati et al., 2019) (CF3) approximate expansions based on the quasi-exact implicit (QEI) formulation proposed by Haverkamp et al. (1994). Note that the QEI model addresses the case of 1D water infiltration and was extended to the case of water infiltration through discs (three-dimensional [3D] axisymmetric geometry) by Smettem et al. (1994).

Core Ideas

- A simplified version of the CTM is proposed to estimate the S and K_s from a 1D infiltration curve.
- The SCTM is nearly as accurate as the original CTM in prediction of S and K_s .
- The SCTM eliminates the necessity of the iteration method used in original CTM.

Although CTM is attractive, providing accurate and simultaneous estimates of S and K_s , the approach suffers from remarkable complexity due to the fact that an iterative procedure is needed to obtain the parameter values and requires programming in, for example, Python, MATLAB, Scilab, and/or VBA. This might hamper a widespread interest and reduce applicability of the CTM. In this paper, we therefore simplified the CTM to eliminate the iterative procedure, making it more practical and simpler with an only slight reduction in the model accuracy. The objective of this paper is to present STCM, a simplified version of the CTM, which is compared with CTM as well the SH, CF2, and CF3 methods. Finally, a simple calculation of the S and K_s in Excel worksheet is presented as supplemental material.

2 | MATERIALS AND METHODS

2.1 | Theoretical background

Following Rahmati et al. (2020), the contribution of capillary- and gravity-driven components to the cumulative infiltration are temporally variable and is illustrated in Figure 1. The contribution of the capillary-driven component shows a maximum at the start of the infiltration process (t close to 0), whereas the contribution of the gravity-driven component is 0.

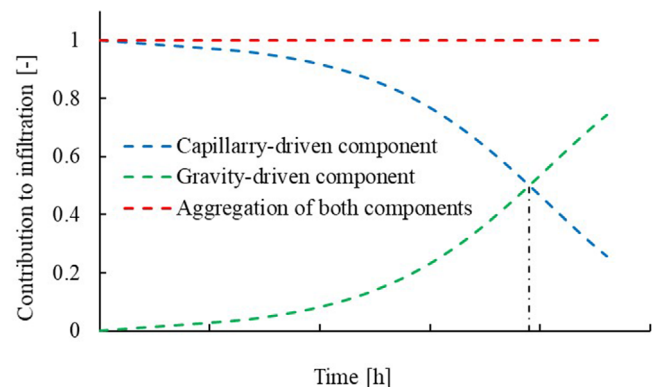


FIGURE 1 Temporal variations of capillary- and gravity-driven components' contributions to cumulative infiltration for the case of an ideal soil (adapted from Rahmati et al., 2020)

By advancing in time, the contribution of the capillary-driven component decreases, leading to symmetrical increase in contribution of the gravity-driven component. The time that both components provide an equal contribution to the cumulative infiltration was defined by Philip (1957) as the gravity time (t_{grav}), and this concept was used by Rahmati et al. (2020) to develop the CTM. They provided the following solutions to predict S and K_s by applying a characteristic time (t_{char}), which falls between 0 and t_{grav} :

$$S = (1 - \omega) \frac{I_{\text{char}}}{\sqrt{t_{\text{char}}}} \quad (1)$$

$$K_s = \frac{-b + \sqrt{b^2 - 4ac}}{2a} \quad (2)$$

where a , b , and c are defined as below:

$$\begin{aligned} a &= \frac{1}{9(1-\omega)} (\beta^2 - \beta + 1) \frac{t_{\text{char}}^2}{I_{\text{char}}} \\ b &= \frac{2-\beta}{3} t_{\text{char}} \\ c &= -\omega I_{\text{char}} \end{aligned} \quad (3)$$

where β (dimensionless) is an integral infiltration constant related to the QEI model (Haverkamp et al., 1994), and t_{char} is linked to t_{grav} as (Rahmati et al., 2020):

$$t_{\text{char}} = \kappa t_{\text{grav}}, \quad \text{where } 0 < \kappa \leq 1 \quad (4)$$

The values of $1 - \omega$ and ω define the contribution of the capillary-driven (sorptivity) and gravity-driven components, respectively, to the cumulative infiltration I_{char} obtained at time t_{char} :

$$1 - \omega = \frac{S \sqrt{t_{\text{char}}}}{I_{\text{char}}} \quad (5)$$

$$\omega = \frac{c_2 t_{\text{char}} + c_3 t_{\text{char}}^{3/2}}{I_{\text{char}}} \quad (6)$$

where

$$\begin{aligned} c_2 &= \frac{2-\beta}{3} K_s \\ c_3 &= (\beta^2 - \beta + 1) \frac{K_s^2}{9S} \end{aligned} \quad (7)$$

To obtain the above solutions, Rahmati et al. (2020) considered the three first components of the approximate expansion of the QEI model for the bulk infiltration by demonstrating that the other terms of the expansion are negligible. Hereafter, the capillary- and gravity-driven components, respectively, refer to the first and the sum of the remaining terms of three-

term approximate expansion of the QEI model (Haverkamp et al., 1994).

In CTM proposed by Rahmati et al. (2020), an iterative procedure is used to determine ω , as well as $t_{\text{char}} - I_{\text{char}}$ set from a measured infiltration curve. To do this, they equalized the $t_{\text{char}} - I_{\text{char}}$ set to different data points of the measured infiltration curve and examined the contribution of the capillary-driven component (W_1) in the vicinity of $t = 0$ where W_1 is defined as below (Rahmati et al., 2020):

$$W_1(t) = \frac{S \sqrt{t}}{I(t)} \quad (8)$$

In the case of $\lim_{t \rightarrow 0} W_1(t) = 1$, the selected datapoint for $t_{\text{char}} - I_{\text{char}}$ is correct and S and K_s can be identified. Otherwise [i.e., $\lim_{t \rightarrow 0} W_1(t) \neq 1$], the next data point is considered for $t_{\text{char}} - I_{\text{char}}$, the procedure is run, and the $\lim_{t \rightarrow 0} W_1(t)$ is checked again. The procedure starts with an initial value of $\omega = 1/2$, corresponding to $t_{\text{char}} = t_{\text{grav}}$. If no correct set of $t_{\text{char}} - I_{\text{char}}$ set is found when all datapoints of the infiltration curve are checked, the maximum experimental time is expected to be lower than t_{grav} . In that case, ω is decreased by small increment (e.g., 0.001), and the above procedure is repeated and ω is decreased until a correct set of $t_{\text{char}} - I_{\text{char}}$ can be found.

To eliminate the necessity of the iterative procedure, we rely on the time independency of the prediction of S with the iterative procedure. In fact, since the CTM predictions of S are independent of the infiltration duration (Rahmati et al., 2020), one can simply choose the latest available data point to define the $t_{\text{char}} - I_{\text{char}}$ set and then predict S by changing ω to achieve $\lim_{t \rightarrow 0} W_1(t) = 1$. By doing so, the necessity for iterative procedure is eliminated.

The correctness of the procedure outlined above can be shown mathematically by setting $t_{\text{char}} = t_{\text{end}}$ and $I_{\text{char}} = I_{\text{end}}$ in Equation 1:

$$S = (1 - \omega) \frac{I_{\text{end}}}{\sqrt{t_{\text{end}}}} \quad (9)$$

where a correct estimate of ω is needed for accurate estimation of S from the above equation.

As mentioned above, the contribution of the capillary-driven component (W_1) on infiltration at any time, t , can be calculated from Equation 8. Substituting S in Equation 8 using Equation 9, we obtain

$$W_1(t) = (1 - \omega) \frac{I_{\text{end}}}{\sqrt{t_{\text{end}}}} \frac{\sqrt{t}}{I(t)} \quad (10)$$

From the above equation, we can estimate ω by knowing that in the case of correct estimate of ω , W_1 will approach unity in the vicinity of the $t = 0$, where

$$\lim_{t \rightarrow 0} W_1(t) = 1 \Rightarrow \lim_{t \rightarrow 0} (1 - \omega) \frac{I_{\text{end}} \sqrt{t}}{\sqrt{t_{\text{end}}} I(t)} = 1 \quad (11)$$

In the case $t = 0$, no solution for the ratio $\sqrt{t}/I(t)$ can be found. This can be solved by using either a t value very close to 0 (e.g., $t = 1$ s), or the first nonzero value of t in the infiltration curve. If we assume that all measured and simulated infiltration curves start at time $t_1 = 0$ at the first datapoint, then the $t_2 - I_2$ set can be the best choice to determine the limit in Equation 11. We can then simply rewrite the above equation as

$$(1 - \omega) \frac{I_{\text{end}} \sqrt{t_2}}{\sqrt{t_{\text{end}}} I_2} = 1 \quad (12)$$

The rearrangement of the above equation gives a correct estimate of the ω :

$$\omega = 1 - \frac{I_2}{I_{\text{end}}} \sqrt{\frac{t_{\text{end}}}{t_2}} \quad (13)$$

By replacing ω in Equation 9 using Equation 13, we can simplify Equation 9 to redefine the final solution for calculating S as

$$S = \frac{I_2}{\sqrt{t_2}} \quad (14)$$

The same procedure is applied to determine K_s . In a similar manner, we calculated the contribution of the gravity-driven component, $W_2(t)$, at different points in time, as below:

$$W_2(t) = \frac{c_2 t + c_3 t^{3/2}}{I} \quad (15)$$

where c_2 and c_3 are defined by Equation 7 considering the estimates of S defined by Equation 14, and β can be set equal to 0.6, as suggested by Haverkamp et al. (1994), or a soil-dependent β can be used as suggested by Lassabatere et al. (2009). However, independent studies (Latorre et al., 2015, 2018; Rahmati et al., 2019, 2020) have shown that the choice of the value of β had only a slight effect on estimating S and K_s , suggesting that we can assume a constant β value of 0.6.

According to Equation 15, we can estimate K_s using the fact that $W_2(t)$ will approach ω at $t = t_{\text{end}}$. Note that the value of ω was computed from the cumulative infiltration value at the latest datapoint in measured infiltration curve with $t_{\text{char}} = t_{\text{end}}$ and the knowledge of sorptivity. This can be written as below:

$$\lim_{t \rightarrow t_{\text{end}}} \frac{c_2 t + c_3 t^{3/2}}{I} = \omega \quad (16)$$

By replacing ω from Equation 13 and using the $t_{\text{end}} - I_{\text{end}}$ set, we can rewrite the above equation as below:

$$\frac{c_2 t_{\text{end}} + c_3 t_{\text{end}}^{3/2}}{I_{\text{end}}} = 1 - \frac{I_2}{I_{\text{end}}} \sqrt{\frac{t_{\text{end}}}{t_2}} \quad (17)$$

Writing Equation 17 in terms of K_s leads to:

$$a' K_s^2 + b' K_s + c' = 0 \quad (18)$$

where

$$\begin{aligned} a' &= \frac{1}{9} (\beta^2 - \beta + 1) \frac{t_{\text{end}}^2}{I_{\text{end}}} \\ b' &= \frac{2-\beta}{3} I_{\text{end}} \\ c' &= I_2 \sqrt{\frac{t_{\text{end}}}{t_2}} - I_{\text{end}} \end{aligned} \quad (19)$$

Finally, solving for K_s in Equation 18 gives

$$K_s = \frac{-b' + \sqrt{b'^2 - 4a'c'}}{2a'} \quad (20)$$

2.2 | Test data

To test the proposed procedure, we used synthetic infiltration curves simulated by using HYDRUS-1D (Šimůnek et al., 2008, 2016) for 12 USDA soil textural classes provided as supplemental material by Rahmati et al. (2020), as well as experimental data (648 infiltration data) selected from Soil Water Infiltration Global (SWIG) database (Rahmati, Weihermüller, Vanderborght, et al., 2018; Rahmati, Weihermüller, & Vereecken, 2018).

2.2.1 | Synthetic data

To synthesize test data using HYDRUS-1D (Šimůnek et al., 2008, 2016), we used the average soil hydraulic parameters (Table 1) of the van Genuchten (VG) model (van Genuchten, 1980) for all examined soils provided by HYDRUS-1D soil catalog (Carsel & Parrish, 1988). The parameters and conditions applied during the simulation process are summarized in Table 2.

Contrary to Rahmati et al. (2020), who simulated the infiltration process up to 240 h, in this study we limited the simulations to the duration of 24 h, as infiltration measurements rarely last more than 24 h. We also assumed that the water level in the system can be measured with a time interval of 1 min, in line with most experimental devices and protocols (Angulo-Jaramillo et al., 2000, 2016; Pakparvar et al., 2018; Rezaei et al., 2016, 2020). We account for this by rounding up the simulated infiltration time data expressed in minutes to

TABLE 1 Average values of soil hydraulic parameters of van Genuchten (VG) model (van Genuchten, 1980) for water retention curve for examined soil texture classes (Carsel & Parrish, 1988) used as synthetic data, as well as the sorptivity (S) data being obtained from the horizontal infiltration simulation (Rahmati et al., 2020). Note that the shape parameter l is fixed at 1/2 for the hydraulic conductivity

Soil	Parameter								
	θ_r	θ_s	θ_i	α	n	m	K_s	S	β
	cm ³ cm ⁻³		cm ⁻¹				cm h ⁻¹	cm h ^{-1/2}	
Clay	0.068	0.380	0.271	0.008	1.09	0.083	0.20	1.02	1.92
Clay loam	0.095	0.410	0.150	0.019	1.31	0.237	0.26	1.46	1.58
Loam	0.078	0.430	0.088	0.036	1.56	0.359	1.04	2.20	1.27
Loamy sand	0.057	0.410	0.057	0.124	2.28	0.561	14.6	6.22	0.80
Sand	0.045	0.430	0.045	0.145	2.68	0.627	29.7	9.23	0.60
Sandy clay	0.100	0.380	0.170	0.027	1.23	0.187	0.12	0.79	1.70
Sandy clay loam	0.100	0.390	0.111	0.059	1.48	0.324	1.31	1.61	1.36
Sandy loam	0.065	0.410	0.066	0.075	1.89	0.471	4.42	3.84	0.99
Silt	0.034	0.460	0.090	0.016	1.37	0.270	0.25	1.35	1.50
Silt loam	0.067	0.450	0.104	0.020	1.41	0.291	0.45	1.66	1.44
Silt clay	0.070	0.360	0.266	0.005	1.09	0.083	0.02	0.35	1.92
Silty clay loam	0.089	0.430	0.197	0.010	1.23	0.187	0.07	0.53	1.70

Note. θ_s , θ_r , and θ_i , saturated, residual, and initial water contents; α , n , and m , parameters of the van Genuchten (1980) model; K_s , saturated hydraulic conductivity; S , soil sorptivity; β , an infiltration constant defined by Haverkamp et al. (1994).

the nearest integer. Then, we selected the cumulative infiltrations corresponding to each minute increment until the whole, or final, cumulative infiltration is reached.

In addition to original simulated curves, similarly to Rahmati et al. (2020), we also added random noises (considering maximum error values of 5, 10, and 20%) to the original synthetic data to provide an additional dataset with more realistic features for performance evaluation. To get more “realistic” time series data assimilable with the measurement process, we defined the error for the infiltration rate and then propagated it to the cumulative infiltration, as suggested by Rahmati et al. (2020). We first obtained the infiltration rate (i) by differentiating the cumulative infiltration (I) curve with respect to time, and then the random noise was added on the infiltration rates as below (Rahmati et al., 2020):

$$i_{\text{noised}} = i + r\sigma \quad (21)$$

$$\sigma = ei \quad (22)$$

where i_{noised} , r , σ , and e , respectively, are the noised infiltration rate vectors, a random number between -1 and 1 picked from normal distribution, the vector of standard deviations, and the magnitude of error considered in analysis. We applied three different e values of 0.05, 0.1, and 0.2, indicating an error of 5, 10, and 20%, respectively. Finally, we integrated the noised infiltration rate vectors (i_{noised}) to calculate the noised cumulative infiltration (I_{noised}) curve as below (Rahmati et al., 2020):

$$I_{\text{noised}}(j) = I_{\text{noised}}(j-1) + i_{\text{noised}}(j) \times [t(j) - t(j-1)] \quad (23)$$

where $j = (1, 2, \dots, n)$ refers to points in infiltration curves.

True or known values of K_s for synthetic data are taken from HYDRUS-1D soil catalog (Carsel & Parrish, 1988), whereas we inferred the true or known values of S by numerically integrating Boltzmann variable, $\lambda(\theta)$, simulated by HYDRUS-1D for infiltration without gravity (Philip, 1957):

$$S = \int_{\theta_i}^{\theta_s} \lambda(\theta) d\theta \quad (24)$$

where θ_i [$L^3 L^{-3}$] and θ_s [$L^3 L^{-3}$] are the initial and saturated volumetric water contents, respectively, and $\lambda(\theta)$ [$L T^{-1/2}$] is defined as

$$\lambda(\theta) = Z(\theta, t)t^{-1/2} \quad (25)$$

where the characteristic function $Z(\theta, t)$ quantifies the depth at which the volumetric water content equates to θ at time t . As such, the values of K_s and S can be considered as utterly known.

2.2.2 | Experimental data

As experimental data, the 1D infiltration data available in the SWIG database (Rahmati, Weihermüller, Vanderborght, et al., 2018; Rahmati, Weihermüller, & Vereecken, 2018) were used to verify the proposed methodology. The selected 1D

infiltration data from SWIG database were obtained from infiltration experiments using a zero water potential imposed at the surface. Overall, we selected 648 infiltration curves for final analysis.

In the case of experimental data, we inferred the benchmark S and K_s values by fitting experimental cumulative infiltrations to the QEI model of Haverkamp et al. (1994) using the online website developed by Latorre et al. (2015): <http://swi.csic.es/infiltration-map/>. The website was initially developed to estimate hydraulic properties from disc infiltrometer 3D infiltration curves (Latorre et al., 2015), making use of the extension of the QEI model to 3D proposed by Smettem et al. (1994). It also includes the fit of the QEI model on 1D experimental infiltration curves. In this study, we considered these values of S and K_s as the benchmark for the following reasons. Firstly, the SWIG database does not provide S values for the selected soils, as that parameter is not measured in field campaigns. Secondly, even for K_s that may be measurable, it is not only reported for a limited number of selected soils, but even the measured K_s values are not representative of the real soil behaviors under infiltration measurement conditions. Several investigations have already shown that K_s values measured in small cylinders significantly differ from those obtained from infiltration measurements because sampling procedures do not ensure the representativeness of samples and may ignore processes like preferential flow that may drive infiltration on the field. Such inconsistency has already confirmed by the analysis of SWIG database (Rahmati, Weihermüller, Vanderborght, et al., 2018).

2.3 | Model comparisons

We compared SCTM with the original CTM (Rahmati et al., 2020), the Sharma et al. (1980) method (SH), and a non-linear curve-fitting method (Bonell & Williams, 1986; Britow & Savage, 1987; Marquardt, 1963; Vandervaere et al., 2000) with two- (CF2, Equation 26) and three-term (CF3, Equation 27) equations, regarding their ability to estimate K_s and S .

$$I(t) = S\sqrt{t} + \frac{2-\beta}{3}K_s t \quad (26)$$

$$I(t) = S\sqrt{t} + \frac{2-\beta}{3}K_s t + \frac{1}{9}(\beta^2 - \beta + 1)\frac{K_s^2}{S}t^{3/2} \quad (27)$$

where $\beta = 0.6$.

In the case of SH method, we estimated S by linear fitting of I vs. \sqrt{t} for data points shorter than 30 min, as suggested by Rahmati et al. (2020). In this approach, the slope provides S when the intercept is set equal to 0. For K_s predictions, we set

TABLE 2 Parameters and conditions applied in HYDRUS-1D to generate the synthetic numerical data (Rahmati et al., 2020)

Simulation parameter	Applied condition
Soil profile depth	200 cm
Boundary condition	
Upper (soil surface)	A zero-pressure head
Lower (bottom of the soil profile)	Free drainage
Soil homogeneity	Homogeneous
Node numbers for discretization	401
Simulation time	24 h
Spatial discretization resolution	
First node	10^{-6} cm
Last node	1 cm
Mode	Increasing by depth
Accuracy check	Based on Boltzmann transform
Employment of internal interpolation tables	Disabled
Hydraulic model	
$n > 1.2$	VG
$n < 1.2$	Modified VG with an air-entry value of -2 cm

Note. n , parameter of van Genuchten (1980) model; VG, van Genuchten (1980) model.

it to be $K_s = \lim_{t \rightarrow t_{\text{end}}} (\Delta I / \Delta t)$. In the case of CF2 and CF3, the “Isqnonlin” function is used for the fit and the optimization of S and K_s .

2.4 | Statistical analysis and evaluation of the estimated hydraulic parameters

The accuracy of the SCTM and the other selected methods was evaluated using the RMSE and Nash and Sutcliffe (1970), E , criteria between measured and predicted K_s and S values:

$$\text{RMSE} = \sqrt{\frac{\sum (X_m - X_p)^2}{n}} \quad (28)$$

$$E = 1 - \frac{\sum (X_m - X_p)^2}{\sum (X_m - \bar{X}_m)^2} \quad (29)$$

where X_m and X_p are the logarithmic values of known and predicted parameters (S and/or K_s), respectively. The values of RMSE and E near 0 and unity, respectively, denote a great accuracy.

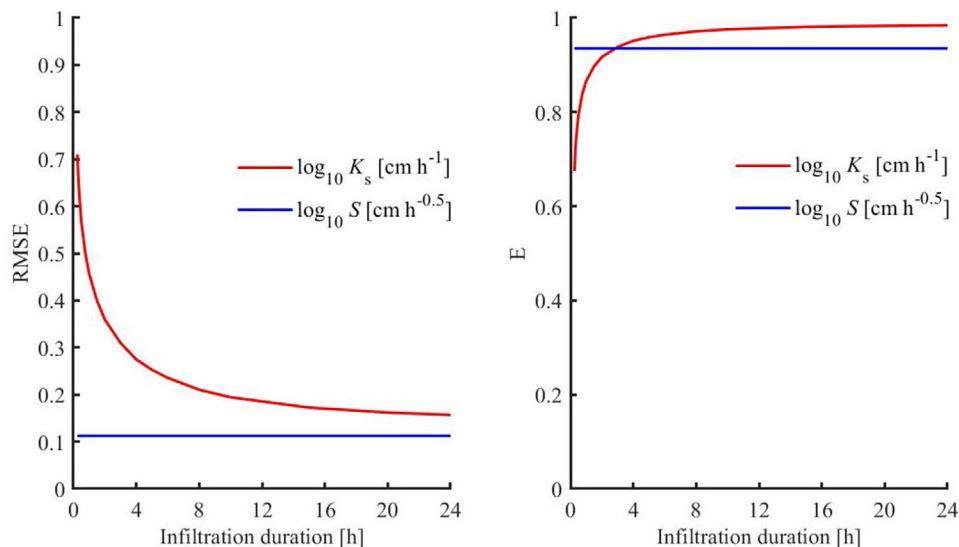


FIGURE 2 RMSE, and Nash and Sutcliffe (1970), E , criteria between true or known and predicted values of saturated hydraulic conductivity, K_s , and sorptivity, S , using the simplified characteristic time method (SCTM) over synthetic data

For the assessment and comparisons of the above methods, we used synthetic infiltration curves with a duration between 15 min and 10 h, corresponding to typical infiltration experiments (Angulo-Jaramillo et al., 2000; Rahmati, Weihermüller, Vanderborght, et al., 2018; Rahmati, Weihermüller, & Vereecken, 2018).

A quantile–quantile (q–q) plot was used to examine graphically if both predicted and true (known) or benchmark populations could be fitted with the same distribution (Wilk & Gnanadesikan, 1968). In other words, from a statistical point of view, a probability q–q plot is a graphical method aimed to compare two probability distributions of two different populations by plotting their quantiles against each other (Wilk & Gnanadesikan, 1968). A vector of 5, 25, 50, 75, and 95 probability levels was used to produce q–q plots.

3 | RESULTS AND DISCUSSION

In this section, we use the synthetic and real data to analyze important features of the SCTM, including the dependence of the accuracy in estimating S and K_s on infiltration duration, the impact of experimental errors on SCTM's accuracy in estimating S and K_s , and its applicability to real experimental data.

3.1 | Performance of SCTM as a function of experimental duration

We evaluated the performance of SCTM using error-free synthetic and experimental data in function of infiltration duration. For that purpose, the synthetic data were truncated

to have different durations of 15 min to 24 h, while the entire curves of experimental data were used for performance evaluation and considered as the benchmark. As shown in Figure 2 and Table 3, the proposed method provided accurate estimates of S and K_s when applied to synthetic data lasting from 15 min to 24 h. The accuracy of the method in estimating S is time independent, as it always uses the second data point of the cumulative infiltration curve to predict S . Although the method leads to a time-dependent accuracy for K_s predictions, it has relatively high accuracy for all infiltration durations lasting for 15 min up to 24 h, showing E values higher than 0.7 and RMSE values lower than 0.7 cm h^{-1} (Figure 2). The need for longer time series stems from the fact that the method works better when the steady-state regime is included in the estimation procedure as in this case, the gravity time t_{grav} is included in the infiltration dataset, and $\omega = 0.5$. Figure 3 shows linear q–q plots of the quantiles of the true and predicted K_s and S , indicating that both samples come from the same log-normal distributions.

Applying the proposed method over experimental data, we found high accuracies in estimating S and K_s as shown in Table 3 and Figure 4, showing RMSE values of 0.64 cm h^{-1} and $0.35 \text{ cm h}^{-1/2}$ and E values of 0.81 and 0.73, in the case of K_s and S predictions, respectively. We also computed the order of magnitudes of difference between predicted and true or known values of K_s (ΔK) and S (ΔS), and a histogram was produced (Figure 5). As seen from Figure 5, overall, more than 86 and 94% of soils show a difference, with order of magnitude of -1 to 1 in the case of K_s and S , respectively. In a similar manner to synthetic data, Figure 6 also shows a linear q–q plot of the quantiles of the benchmark and predicted K_s and S for the experimental data, indicating that both samples come from the same log-normal distributions.

TABLE 3 Average RMSE and Nash and Sutcliffe (1970), E , criteria between true or known and predicted values of saturated hydraulic conductivity, K_s , and sorptivity, S , over both synthetic and experimental datasets containing 12 (synthetic) and 648 (experiments) number of data (n)

Criterion	Synthetic data ($n = 12$)		Experimental data ($n = 648$)	
	$\log_{10}(K_s)$	$\log_{10}(S)$	$\log_{10}(K_s)$	$\log_{10}(S)$
	cm h^{-1}	$\text{cm h}^{-1/2}$	cm h^{-1}	$\text{cm h}^{-1/2}$
RMSE	0.350 ± 0.178	0.112 ± 0.000	0.639	0.346
E	0.902 ± 0.096	0.935 ± 0.000	0.806	0.726

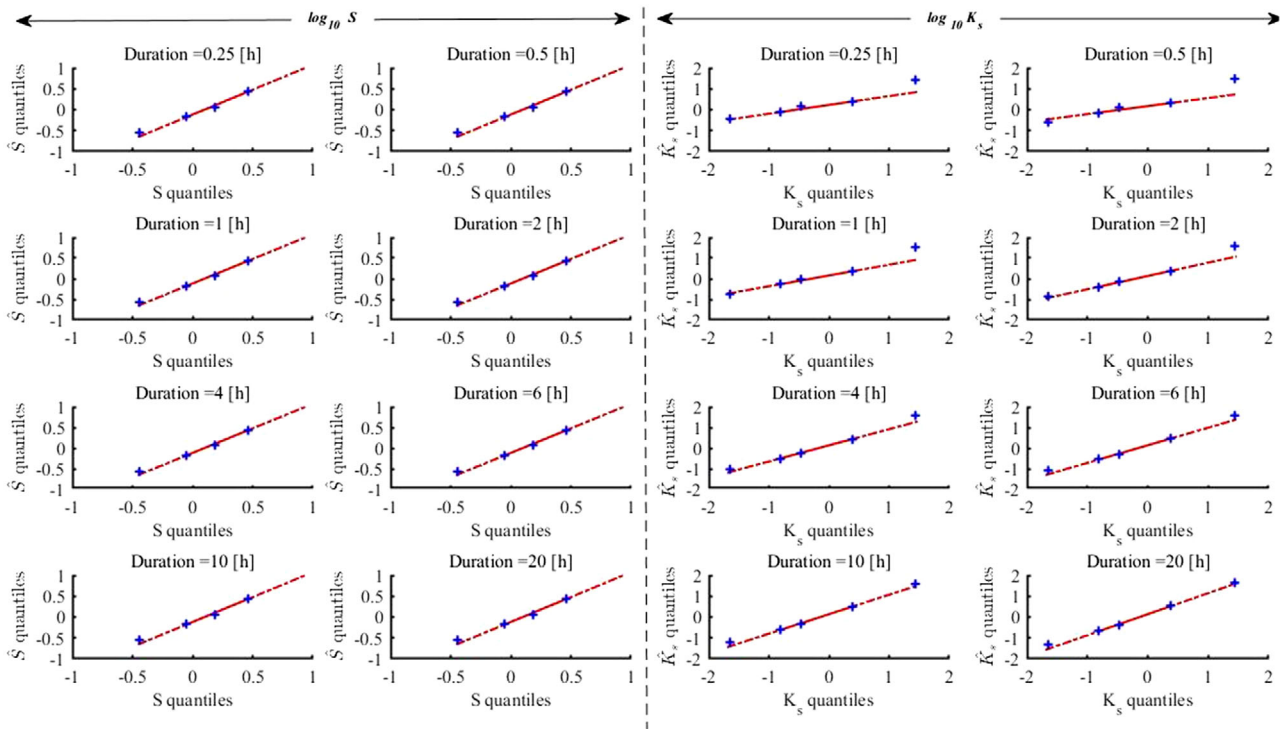


FIGURE 3 Quantile–quantile plots of quantiles (5, 25, 50, 75, and 95%) of true and predicted values of sorptivity (S and \hat{S}) and saturated hydraulic conductivity (K_s and \hat{K}_s) for synthetic data. Both true and predicted values are shown in logarithmic scale

3.2 | Models comparison using error-free and noised synthetic infiltration curves

We compared the accuracy of the SCTM in estimating S and K_s with estimates obtained from CTM as well as SH, CF2, and CF3. In addition to the original error-free data, random noises were added to synthetic infiltration data, and predictions were repeated to evaluate the effects of error in infiltration data on predictions. Table 4 reports the average RMSE and E values obtained between known and predicted values of K_s and S for all the methods and data types.

Comparing SCTM with CTM shows that in the case of error-free data, the SCTM works even better than CTM for K_s predictions, with an average RMSE value of $0.38 \pm 0.19 \text{ cm h}^{-1}$ vs. $0.57 \pm 0.20 \text{ cm h}^{-1}$ and an E value of 0.89 ± 0.11 vs. 0.77 ± 0.16 . Both methods (SCTM and CTM) have similar accuracy for S predictions, with an average RMSE value of $0.11 \text{ cm h}^{-1/2}$ and E value of 0.94.

Overall, CF3 was found to be the best at estimating both S and K_s when using error-free data, with an average RMSE value of $0.28 \pm 0.10 \text{ cm h}^{-1}$ for K_s predictions and $0.05 \pm 0.03 \text{ cm h}^{-1/2}$ for S predictions. In the case of noised data, both CF2 and CF3 resulted in less accurate predictions of K_s , showing average RMSE values higher than 1.73 cm h^{-1} and E values lower than 0, though they still outperformed (particularly CF3) in the case of S predictions. The CTM was better than other methods for K_s predictions when applied to noised data, showing average RMSE values lower than $0.59 \text{ cm h}^{-1/2}$ and E values higher than 0.77. Although, the SCTM ranked third after CTM and SH for K_s prediction, it still has a relatively high accuracy and satisfactory predicted K_s , showing an average RMSE value lower than 0.75 cm h^{-1} and E value higher than 0.61. All applied methods were accurate enough for S predictions, showing E values higher than 0.85 and RMSE values lower than $0.17 \text{ cm h}^{-1/2}$. In other words, CTM and SCTM methods were quite competitive when dealing

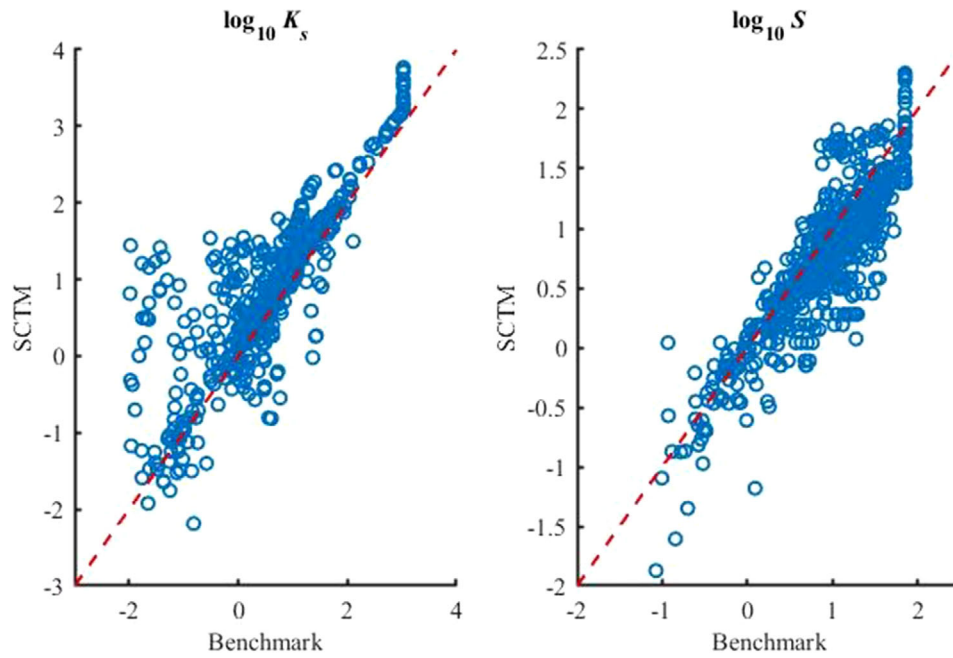


FIGURE 4 Predicted values of saturated hydraulic conductivity, K_s (left), and sorptivity, S (right), vs. true or known values (benchmark) using the simplified characteristic time method (SCTM) for experimental data

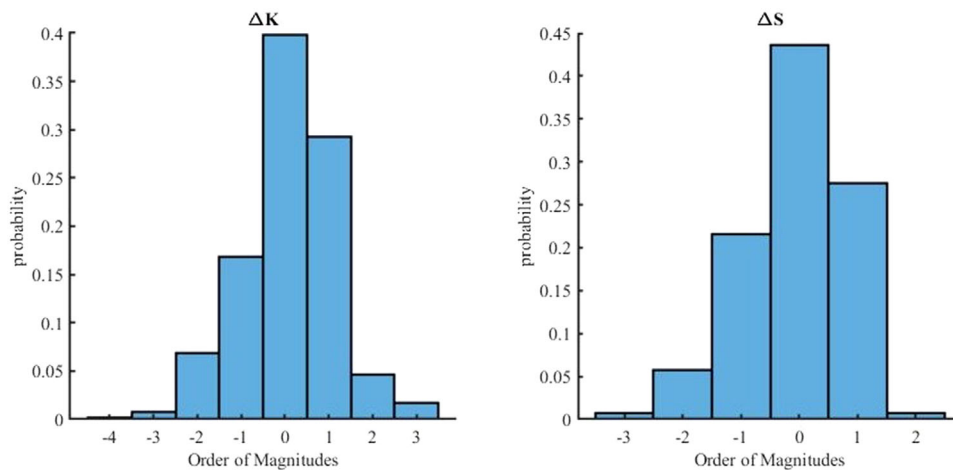


FIGURE 5 Histogram of order of magnitudes of differences of true or known (benchmark) and SCTM-predicted values of saturated hydraulic conductivity, ΔK (left), and sorptivity, ΔS (right), over experimental data. The SCTM implies for simplified characteristic time method

with noised data, whereas CF2 and CF3 failed to deal with data contaminated with noise. These two methods should be avoided when using experimental data to estimate S and K_s .

3.3 | Models comparison using experimental data

In this section, we evaluated the accuracy of the SCTM in comparison with the other methods when applied to experimental data. The results are illustrated in Figures 7 and 8

and are summarized in Table 5. The results revealed that the accuracy of the SCTM in estimating S and K_s is comparable with the accuracy of the CTM, as well as the classical method of SH. It showed a slightly lower accuracy compared with CTM and SH, with an RMSE value of 0.64 cm h^{-1} for K_s predictions and $0.35 \text{ cm h}^{-1/2}$ for S predictions. Both CF2 and CF3 methods failed in accurate predictions of K_s , showing an RMSE value of around 2 cm h^{-1} and negative E values. However, CF3 placed second in the rank for S predictions, showing an RMSE value of $0.27 \text{ cm h}^{-1/2}$ and E value of 0.83.

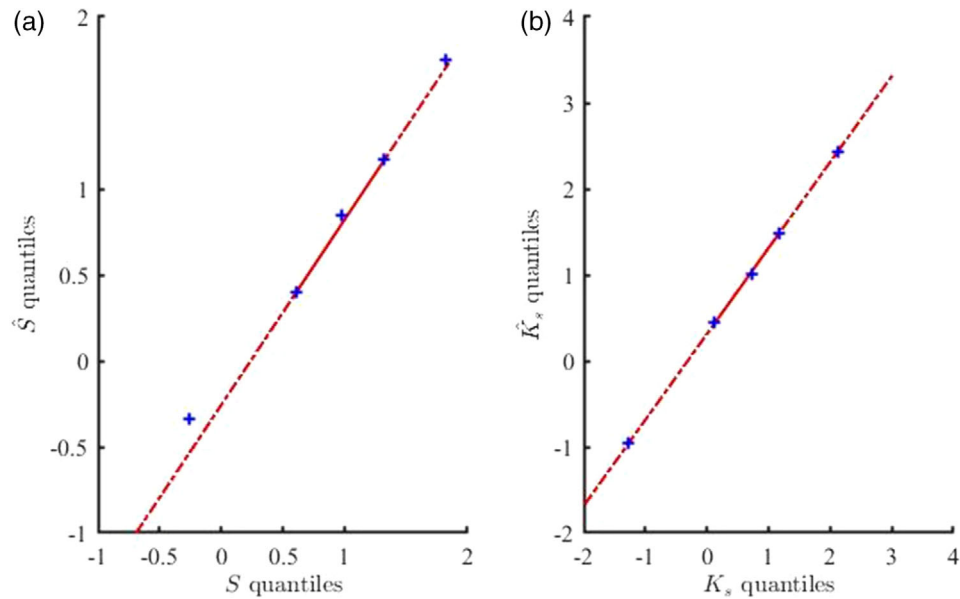


FIGURE 6 Quantile–quantile plots of quantiles (5, 25, 50, 75, and 95%) of true and predicted values of (a) sorptivity (S and \hat{S}) and (b) saturated hydraulic conductivity (K_s and \hat{K}_s) for experimental data. Both true and predicted values are shown in logarithmic scale

TABLE 4 Average RMSE between known and predicted saturated hydraulic conductivity, K_s , and sorptivity, S , values using the simplified (SCTM) and original (CTM) characteristic time method, Sharma method (SH), and nonlinear curve fitting method of two- (CF2) and three-term (CF3) equations over original (error-free) and noised synthetic data for all soils

Data	Method	RMSE		E	
		$\log_{10}(K_s)$ cm h ⁻¹	$\log_{10}(S)$ cm h ^{-1/2}	$\log_{10}(K_s)$ cm h ⁻¹	$\log_{10}(S)$ cm h ^{-1/2}
Error-free data	SCTM	0.376 ± 0.187	0.112 ± 0.000	0.889 ± 0.107	0.935 ± 0.000
	CTM	0.568 ± 0.200	0.107 ± 0.000	0.769 ± 0.160	0.941 ± 0.000
	SH	0.552 ± 0.220	0.122 ± 0.015	0.776 ± 0.173	0.923 ± 0.016
	CF2	0.315 ± 0.099	0.156 ± 0.072	0.931 ± 0.045	0.851 ± 0.119
	CF3	0.282 ± 0.095	0.053 ± 0.026	0.944 ± 0.039	0.983 ± 0.014
Noised data (5%)	SCTM	0.749 ± 0.209	0.147 ± 0.000	0.613 ± 0.221	0.889 ± 0.000
	CTM	0.463 ± 0.202	0.123 ± 0.003	0.839 ± 0.131	0.922 ± 0.003
	SH	0.585 ± 0.241	0.130 ± 0.012	0.746 ± 0.202	0.912 ± 0.015
	CF2	1.927 ± 0.668	0.159 ± 0.069	-1.650 ± 1.83	0.847 ± 0.119
	CF3	1.958 ± 0.512	0.062 ± 0.019	-1.624 ± 1.22	0.978 ± 0.012
Noised data (10%)	SCTM	0.747 ± 0.213	0.147 ± 0.000	0.614 ± 0.225	0.889 ± 0.000
	CTM	0.462 ± 0.199	0.123 ± 0.003	0.840 ± 0.131	0.921 ± 0.004
	SH	0.585 ± 0.243	0.131 ± 0.013	0.746 ± 0.204	0.910 ± 0.015
	CF2	1.733 ± 0.435	0.159 ± 0.066	-1.048 ± 0.98	0.845 ± 0.113
	CF3	1.946 ± 0.448	0.062 ± 0.019	-1.558 ± 1.04	0.979 ± 0.012
Noised data (20%)	SCTM	0.753 ± 0.209	0.147 ± 0.000	0.609 ± 0.221	0.889 ± 0.000
	CTM	0.585 ± 0.118	0.123 ± 0.003	0.771 ± 0.094	0.922 ± 0.004
	SH	0.591 ± 0.243	0.130 ± 0.012	0.741 ± 0.206	0.913 ± 0.014
	CF2	1.751 ± 0.475	0.172 ± 0.064	-1.109 ± 1.27	0.828 ± 0.109
	CF3	2.046 ± 0.569	0.064 ± 0.018	-1.886 ± 1.54	0.977 ± 0.102

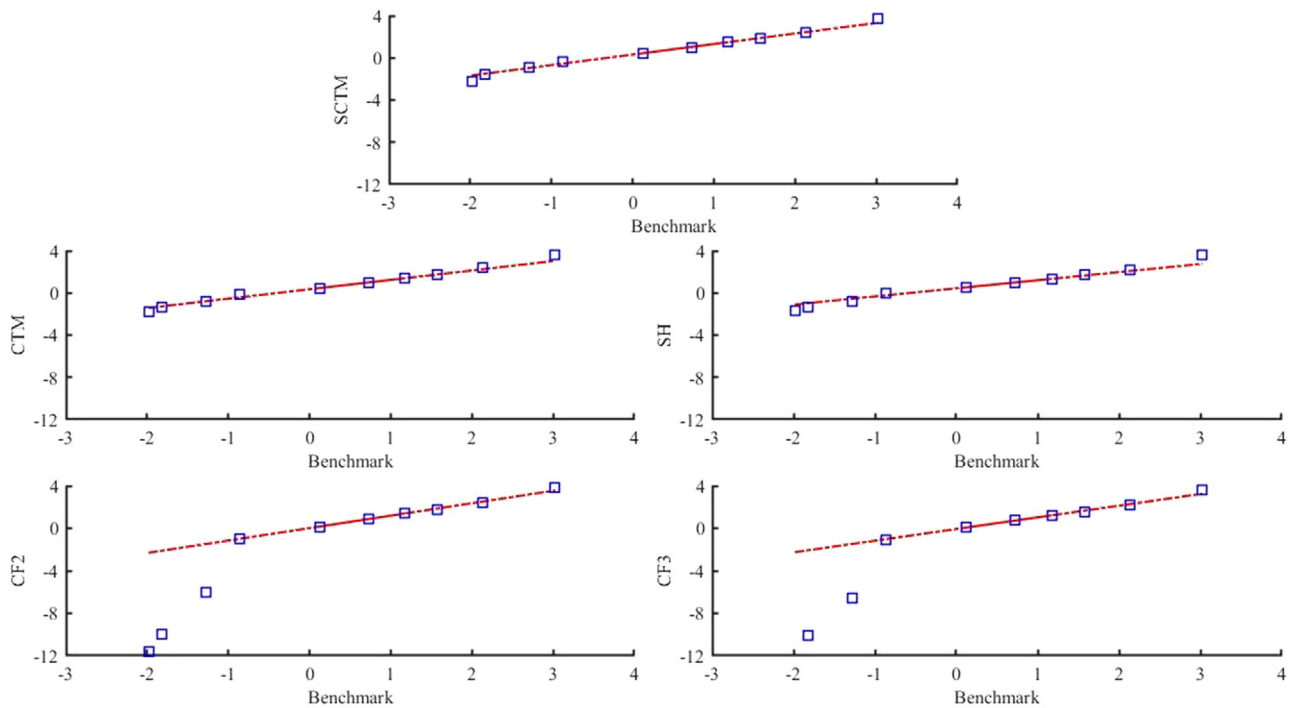


FIGURE 7 Quantile–quantile plots of quantiles (0, 1, 5, 10, 25, 50, 75, 90, 95, and 100%) of logarithms of benchmark and predicted saturated hydraulic conductivity, K_s , values using the simplified (SCTM) and original (CTM) characteristic time method and Sharma et al. (1980) (SH) method, as well as curve fitting methods of two- (CF2) and three-term (CF3) equations over the data selected from the Soil Water Infiltration Global (SWIG) database

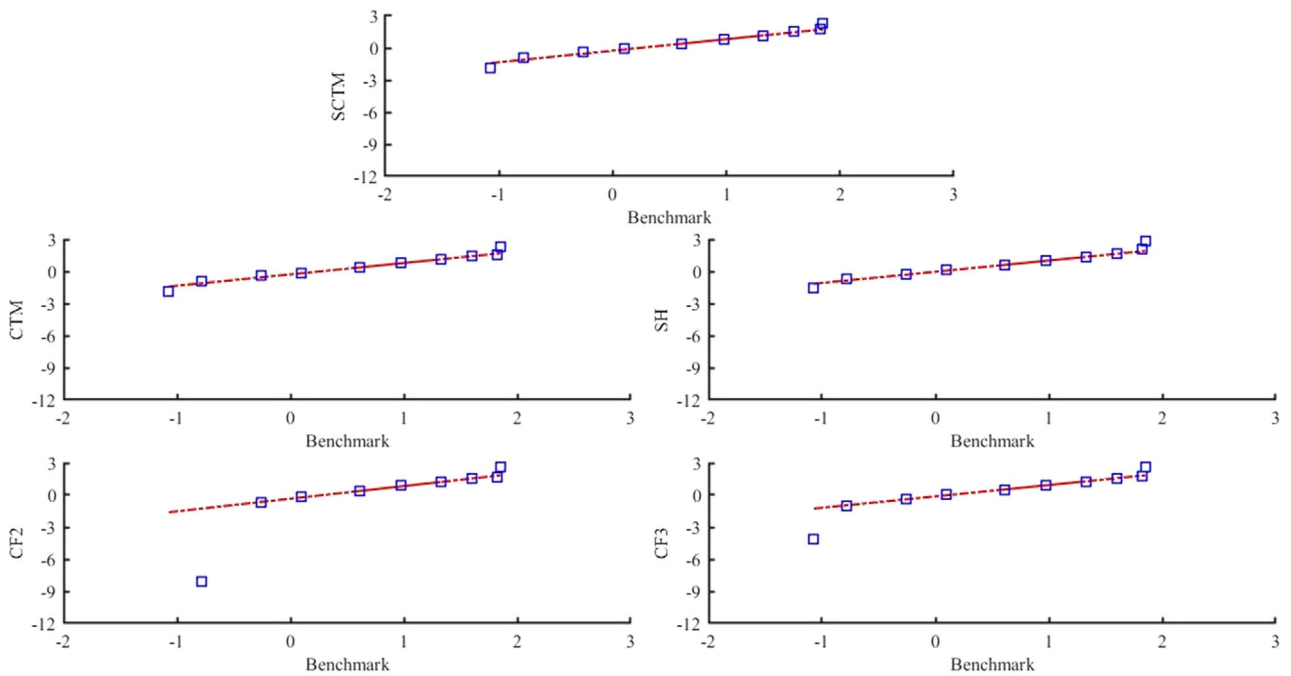


FIGURE 8 Quantile–quantile plots of quantiles (0, 1, 5, 10, 25, 50, 75, 90, 95, and 100%) of logarithms of the benchmark and predicted sorptivity, S , values using the simplified (SCTM) and original (CTM) characteristic time method and Sharma et al. (1980) (SH) method, as well as curve fitting methods of two- (CF2) and three-term (CF3) equations over the data selected from the Soil Water Infiltration Global (SWIG) database

TABLE 5 Average RMSE and Nash and Sutcliffe (1970), E , criteria between known and predicted saturated hydraulic conductivity, K_s , and sorptivity, S , values using the simplified (SCTM) and original (CTM) characteristic time method, as well as the Sharma method (SH), and nonlinear curve fitting method of two- (CF2) and three-term (CF3) equations over experimental data of the Soil Water Infiltration Global (SWIG) database

Criterion	Method	$\log_{10}(K_s)$	$\log_{10}(S)$
		cm h ⁻¹	cm h ^{-1/2}
RMSE	SCTM	0.639	0.346
	CTM	0.511	0.320
	SH	0.514	0.178
	CF2	1.963	1.320
	CF3	2.039	0.272
E	SCTM	0.806	0.726
	CTM	0.876	0.766
	SH	0.875	0.928
	CF2	-0.833	-2.995
	CF3	-0.977	0.830

The SCTM, CTM, and SH methods not only provided higher accuracy in S and K_s predictions compared with CF2 and CF3, but they also provided a constrained fitting of the parameters ensuring that predictions will be within the physically meaningful range. Conversely, this is not the case for CF2 and CF3.

4 | CONCLUSIONS

In this paper, we simplified the characteristic time method (CTM), which was proposed based on the concept of characteristic time (t_{char}) to estimate the soil sorptivity, S , and the saturated hydraulic conductivity, K_s . A novel method, coined SCTM (simplified characteristic time method), maintains all the features of the original CTM but does not require the complex iteration procedure needed to estimate S and K_s . The SCTM uses the first point of the cumulative infiltration to estimate S and the last data point to predict K_s , rather than iterating over all data points, as is done in CTM. The SCTM performance and accuracy was analyzed using simulated and experimental infiltration curves and compared with CTM, as well as typically used methods in the literature, including nonlinear curve fitting of two- (CF2) and three-term (CF3) equations, and the methods proposed by Sharma et al. (1980) (SH). The HYDRUS-1D-simulated synthetic infiltration curves provided as supplemental material by Rahmati et al. (2020), as well as experimental data selected from the SWIG database (Rahmati, Weihermüller, Vanderborght, et al., 2018; Rahmati, Weihermüller, & Vereecken, 2018), were used to evaluate the applied methods performances. The SCTM

provided accurate predictions of K_s and S , being comparable with the original CTM when tested against both synthetic and experimental data. The SCTM benefits from all advantages of the original CTM method, while it is much simpler than the original method and more practical. The SCTM was found to be applicable to any infiltration duration within a typical time window used for infiltration experiments (15 min to 10 h), and even up to 24 h.

AUTHOR CONTRIBUTIONS

Mehdi Rahmati: Conceptualization; Data curation; Formal analysis; Investigation; Methodology; Validation; Visualization; Writing-original draft; Writing-review & editing. Meisam Rezaei: Writing-original draft; Writing-review & editing. Laurent Lassabatere: Writing-original draft; Writing-review & editing. Renato Morbidelli: Writing-original draft; Writing-review & editing. Harry Vereecken: Project administration; Supervision; Writing-original draft; Writing-review & editing.

CONFLICT OF INTEREST

The authors declare no conflict of interest.

REFERENCES

- Angulo-Jaramillo, R., Bagarello, V., Iovino, M., & Lassabatere, L. (2016). *Infiltration measurements for soil hydraulic characterization*. Springer.
- Angulo-Jaramillo, R., Vandervaere, J. P., Roulier, S., Thony, J. L., Gaudet, J. P., & Vauclin, M., (2000). Field measurement of soil surface hydraulic properties by disc and ring infiltrometers: A review and recent developments. *Soil and Tillage Research*, 55, 1–29. [https://doi.org/10.1016/S0167-1987\(00\)00098-2](https://doi.org/10.1016/S0167-1987(00)00098-2)
- Beven, K., & Freer, J. (2001). Equifinality, data assimilation, and uncertainty estimation in mechanistic modelling of complex environmental systems using the GLUE methodology. *Journal of Hydrology*, 249, 11–29. [https://doi.org/10.1016/S0022-1694\(01\)00421-8](https://doi.org/10.1016/S0022-1694(01)00421-8)
- Bonell, M., & Williams, J. (1986). The two parameters of the Philip infiltration equation: Their properties and spatial and temporal heterogeneity in a red earth of tropical semi-arid Queensland. *Journal of Hydrology*, 87, 9–31. [https://doi.org/10.1016/0022-1694\(86\)90112-5](https://doi.org/10.1016/0022-1694(86)90112-5)
- Bristow, K. L., & Savage, M. J. (1987). Estimation of parameters for the Philip two-term infiltration equation applied to field soil experiments. *Soil Research*, 25, 369–375. <https://doi.org/10.1071/SR9870369>
- Carsel, R. F., & Parrish, R. S., (1988). Developing joint probability distributions of soil water retention characteristics. *Water Resources Research*, 24, 755–769. <https://doi.org/10.1029/WR024i005p00755>
- Corradini, C., Melone, F., & Smith, R. E. (1997). A unified model for infiltration and redistribution during complex rainfall patterns. *Journal of Hydrology*, 192, 104–124. [https://doi.org/10.1016/S0022-1694\(96\)03110-1](https://doi.org/10.1016/S0022-1694(96)03110-1)
- Green, W. H., & Ampt, G. A. (1911). Studies on soil physics. *Journal of Agricultural Science*, 4, 1–24. <https://doi.org/10.1017/S0021859600001441>
- Haverkamp, R., Ross, P. J., Smettem, K. R. J., & Parlange, J. Y. (1994). Three-dimensional analysis of infiltration from the disc infiltrometer: 2. Physically based infiltration equation. *Water Resources Research*, 30, 2931–2935. <https://doi.org/10.1029/94WR01788>

- Lassabatere, L., Angulo-Jaramillo, R., Soria-Ugalde, J., Šimůnek, J., & Haverkamp, R. (2009). Numerical evaluation of a set of analytical infiltration equations. *Water Resources Research*, 45(12). <https://doi.org/10.1029/2009WR007941>
- Latorre, B., Moret-Fernández, D., Lassabatere, L., Rahmati, M., López, M. V., Angulo-Jaramillo, R., Sorando, R., Comín, F., & Jiménez, J. J. (2018). Influence of the β parameter of the Haverkamp model on the transient soil water infiltration curve. *Journal of Hydrology*, 564, 222–229. <https://doi.org/10.1016/j.jhydrol.2018.07.006>
- Latorre, B., Peña, C., Lassabatere, L., Angulo-Jaramillo, R., & Moret-Fernández, D. (2015). Estimate of soil hydraulic properties from disc infiltrometer three-dimensional infiltration curve. Numerical analysis and field application. *Journal of Hydrology*, 527, 1–12. <https://doi.org/10.1016/j.jhydrol.2015.04.015>
- Marquardt, D. W. (1963). An algorithm for least-squares estimation of nonlinear parameters. *Journal of the Society for Industrial and Applied Mathematics*, 11, 431–441. <https://doi.org/10.1137/0111030>
- Nash, J. E., & Sutcliffe, J. V. (1970). River flow forecasting through conceptual models Part I: A discussion of principles. *Journal of Hydrology*, 10, 282–290. [https://doi.org/10.1016/0022-1694\(70\)90255-6](https://doi.org/10.1016/0022-1694(70)90255-6)
- Pakparvar, M., Hashemi, H., Rezaei, M., Cornelis, W. M., Nekooeian, G., & Kowsar, S. A. (2018). Artificial recharge efficiency assessment by soil water balance and modelling approaches in a multi-layered vadose zone in a dry region. *Hydrological Sciences Journal*, 63, 1183–1202. <https://doi.org/10.1080/02626667.2018.1481962>
- Parlange, J. Y., Lisle, I., Braddock, R. D., & Smith, R. E. (1982). The three-parameter infiltration equation. *Soil Science*, 133, 337–341. <https://doi.org/10.1097/00010694-198206000-00001>
- Philip, J. R. (1957). The theory of infiltration: 1. The infiltration equation and its solution. *Soil Science*, 83, 345–358. <https://doi.org/10.1097/00010694-195705000-00002>
- Rahmati, M., Latorre, B., Lassabatere, L., Angulo-Jaramillo, R., & Moret-Fernández, D. (2019). The relevance of Philip theory to Haverkamp quasi-exact implicit analytical formulation and its uses to predict soil hydraulic properties. *Journal of Hydrology*, 570, 816–826. <https://doi.org/10.1016/j.jhydrol.2019.01.038>
- Rahmati, M., Vanderborght, J., Šimunek, J., Vrugt, J. A., Moret-Fernández, D., Latorre, B., Lassabatere, L., & Vereecken, H. (2020). Characteristic time and its usage for improving estimation of the soil sorptivity and saturated hydraulic conductivity from one-dimensional infiltration experiments. *Vadose Zone Journal*, 19, e20068. <https://doi.org/10.1002/vzj2.20068>
- Rahmati, M., Weihermüller, L., Vanderborght, J., Pachepsky, Y. A., Mao, L., Sadeghi, S. H., ..., & Vereecken, H. (2018). Development and analysis of the Soil Water Infiltration Global database. *Earth System Science Data*, 10, 1237–1263. <https://doi.org/10.5194/essd-10-1237-2018>
- Rahmati, M., Weihermüller, L., & Vereecken, H. (2018). Soil Water Infiltration Global (SWIG) database. Supplement to Rahmati et al. (Eds.), *Development and analysis of soil water infiltration global database*. PANGAEA. <https://doi.org/10.1594/PANGAEA>
- Rezaei, M., Seuntjens, P., Shahidi, R., Joris, I., Boëne, W., Al-Barri, B., & Cornelis, W. (2016). The relevance of in-situ and laboratory characterization of sandy soil hydraulic properties for soil water simulations. *Journal of Hydrology*, 534, 251–265. <https://doi.org/10.1016/j.jhydrol.2015.12.062>
- Rezaei, M., Shahbazi, K., Shahidi, R., Davatgar, N., Bazargan, K., Rezaei, H., ... & Cornelis, W. (2020). How to relevantly characterize hydraulic properties of saline and sodic soils for water and solute transport simulations. *Journal of Hydrology*. <https://doi.org/10.1016/j.jhydrol.2020.125777> (in press).
- Sharma, M. L., Gander, G. A., & Hunt, C. G. (1980). Spatial variability of infiltration in a watershed. *Journal of Hydrology*, 45, 101–122. [https://doi.org/10.1016/0022-1694\(80\)90008-6](https://doi.org/10.1016/0022-1694(80)90008-6)
- Šimůnek, J., van Genuchten, M. Th., & Šejna, M. (2008). Development and applications of the HYDRUS and STANMOD software packages and related codes. *Vadose Zone Journal*, 7, 587–600. <https://doi.org/10.2136/vzj2007.0077>
- Šimůnek, J., van Genuchten, M. Th., & Šejna, M. (2016). Recent developments and applications of the HYDRUS computer software packages. *Vadose Zone Journal*, 15. <https://doi.org/10.2136/vzj2016.04.0033>
- Smettem, K., Parlange, J., Ross, P., & Haverkamp, R. (1994). Three-dimensional analysis of infiltration from the disc infiltrometer: 1. A capillary-based theory. *Water Resources Research*, 30, 2925–2929. <https://doi.org/10.1029/94WR01787>
- Smiles, D. E., & Knight, J. H. (1976). A note on the use of the Philip infiltration equation. *Soil Research*, 14, 103–108. <https://doi.org/10.1071/SR9760103>
- Swartzendruber, D. (1987). A quasi-solution of Richards' Equation for the downward infiltration of water into soil. *Water Resources Research*, 23, 809–817. <https://doi.org/10.1029/WR023i005p0809>
- van Genuchten, M. Th. (1980). A closed-form equation for predicting the hydraulic conductivity of unsaturated soils. *Soil Science Society of America Journal*, 44, 892–898. <https://doi.org/10.2136/sssaj1980.03615995004400050002x>
- Vandervaere, J. P., Vauclin, M., & Elrick, D. E. (2000). Transient flow from tension infiltrometers I. The two-parameter equation. *Soil Science Society of America Journal*, 64, 1263–1272. <https://doi.org/10.2136/sssaj2000.6441263x>
- Wilk, M. B., & Gnanadesikan, R. (1968). Probability plotting methods for the analysis for the analysis of data. *Biometrika*, 55, 1–17.

SUPPORTING INFORMATION

Additional supporting information may be found online in the Supporting Information section at the end of the article.

How to cite this article: Rahmati M, Rezaei M, Lassabatere L, Morbidelli R, & Vereecken H. (2021). Simplified characteristic time method for accurate estimation of the soil hydraulic parameters from one-dimensional infiltration experiments. *Vadose Zone J.* 2021; 20:e20117. <https://doi.org/10.1002/vzj2.20117>